Journal of Water Resource and Protection, 2024, 16, 1-16
https://www.scirp.org/journal/jwarp
ISSN Online: 1945-3108
ISSN Print: 1945-3094

Fate and Behavior of Tetracycline Resistance Genes in Activated Carbon Adsorption

Sri Anggreini[1], Alma Rizky Aurellya[2], Wenqing Li[1], Fusheng Li[1,3*]

[1]Graduate School of Engineering, Gifu University, Gifu, Japan
[2]Graduate School of Natural Science and Technology, Gifu University, Gifu, Japan
[3]River Basin Research Center, Gifu University, Gifu, Japan
Email: sri.anggreini.c2@s.gifu-u.ac.jp, *li.fusheng.i4@f.gifu-u.ac.jp

How to cite this paper: Anggreini, S., Aurellya, A.R., Li, W.Q. and Li, F.S. (2024) Fate and Behavior of Tetracycline Resistance Genes in Activated Carbon Adsorption. *Journal of Water Resource and Protection*, **16**, 1-16.
https://doi.org/10.4236/jwarp.2024.161001

Received: December 3, 2023
Accepted: January 2, 2024
Published: January 5, 2024

Abstract

The accessibility of tetracycline resistance gene (*tetG*) into the pores of activated carbon (AC), as well as the impact of the pore size distribution (PSD) of AC on the uptake capacity of *tetG*, were investigated using eight types of AC (four coal-based and four wood-based). AC showed the capability to admit *tetG* and the average reduction of *tetG* for coal-based and wood-based ACs at the AC dose of 1 $g \cdot L^{-1}$ was 3.12 log and 3.65 log, respectively. The uptake kinetic analysis showed that the uptake of the gene followed the pseudo-second-order kinetics reaction, and the uptake rate constant for the coal-based and wood-based ACs was in the range of 5.97×10^{-12} - 4.64×10^{-9} and 7.02×10^{-11} - 1.59×10^{-8} copies$\cdot mg^{-1} \cdot min^{-1}$, respectively. The uptake capacity analysis by fitting the obtained experiment data with the Freundlich isotherm model indicated that the uptake constant (K_F) values were 1.71×10^3 – 8.00×10^9 $(copies \cdot g^{-1})^{1-1/n}$ for coal-based ACs and 7.00×10^8 - 3.00×10^{10} $(copies \cdot g^{-1})^{1-1/n}$ for wood-based ones. In addition, the correlation analysis between K_F values and pore volume as well as pore surface at different pore size regions of ACs showed that relatively higher positive correlation was found for pores of 50 - 100 Å, suggesting ACs with more pores in this size region can uptake more *tetG*. The findings of this study are valuable as reference for optimizing the adsorption process regarding antibiotic resistance-related concerns in drinking water treatment.

Keywords

Antibiotic Resistance Genes, Adsorption, Activated Carbon, Drinking Water Treatment

1. Introduction

Antibiotics have been widely used since the 1940s to treat bacterial infections in

humans, livestock, and aquaculture, as well as feed additives in animal husbandry [1]. The overuse of antibiotics has resulted in the proliferation of antibiotic resistance genes (ARGs) in the aquatic environment. ARGs can survive in water even in the absence of selective pressure and spread their antibiotic resistance traits through vertical gene transfer (*i.e.* via cell division) and horizontal gene transfer (*i.e.* via conjugation, transduction, and transformation) [2] [3]. The emergence of ARGs has raised significant concerns due to their potential implications on public health. ARGs can directly impact the effectiveness of antibiotics, which are crucial medications for treating diseases. Bacteria evolve antibiotic resistance to enhance their survival, thus reducing treatment options to treat infections, prolonging illness, increasing healthcare costs, and elevating mortality rates in the human population. Antibiotic resistance has caused more than 25,000, 38,000, 58,000 and 23,000 deaths in the European Union, Thailand, India, and the United States each year, respectively [4]. Nowadays, antibiotic resistance contributes to approximately 700,000 deaths worldwide each year [5]. Antibiotic resistance is expected to produce a significant public health crisis by 2050, resulting in over 10 million deaths and a global cost burden of approximately US$100 trillion [6].

Tetracycline is a frequently utilized antibiotic in humans and animals due to its broad-spectrum activity and low cost [7]. The widespread application of tetracyclines in aquaculture, animal husbandry, and healthcare has led to the spread of tetracycline resistance genes in the environment. Previous studies reported that tetracycline resistance genes were predominantly detected in the aquatic environment [8] [9] [10]. Tetracycline resistance prevalence in certain European countries was observed to be 66.9% and 44.9% for Escherichia coli and Klebsiella (spp.) species, respectively [11]. In addition, WHO has added tetracycline resistance to its priority list of critical antibiotic-resistant bacteria (ARB) in drinking water [6]. Therefore, mitigating and controlling the proliferation of tetracycline resistance genes is essential for ecological safety and human health.

ARGs have been broadly detected in various environmental contexts, including surface water, groundwater, hospital and livestock sewage, as well as wastewater treatment effluents [12] [13] [14] [15]. ARGs originating from different sources will accumulate in the drinking water source and be carried along with raw water to the drinking water treatment plant (DWTP). Nevertheless, DWTP is not able to eliminate ARGs completely, leading to the presence of ARGs in tap water [16]. Thus, there is a possibility of exposure during bathing, cooking, and other uses. The issue of ARGs in drinking water deserves attention because it is closely related to people's daily lives and threatens human health. The understanding of the fate and behavior of ARGs in various treatment processes, including coagulation, sedimentation, sand filtration, chlorination, and activated carbon (AC) adsorption, has not been identified. Concerning the adsorption process, the implications of the adsorption of ARGs on AC have not been well defined. Most studies have reported that granular AC filtration increases the diversity and absolute abundance of ARGs since the biofilm on the AC surface can

act as a nutrient source for ARBs and be an ideal site for the dissemination of ARGs [17] [18]. Meanwhile, powdered AC, which is commonly added to DWTP receiving wells, resulted in a low reduction of ARGs. Previous research reported that the reduction of 27 ARGs by powdered AC in DWTP only reached 0.23 log toward influent concentrations of 1.83×10^9 - 3.51×10^9 copies·L^{-1} [16]. Powdered AC can also increase the spread of ARGs during the recycling of water from drinking water treatment sludge as raw water. ARGs may be able to enter the AC pores and possibly be released from the pores during the recycling process. The released ARGs can transfer their resistance trait to bacteria, leading to the spread of ARGs during the recycling process. Thus, the penetration of ARGs into the pores of AC can cause problems in both granular and powdered AC. This emphasizes the need for comprehensive investigations to elucidate the fate and behavior of ARGs during the adsorption process, which is critical for optimizing water treatment strategies and tackling concerns related to antibiotic resistance.

AC adsorption is widely used in drinking water treatment to remove various contaminants in water due to its larger surface area and pore volume. The uptake of ARGs on AC might be affected by various properties of AC such as total surface area, total pore volume, pore size distribution (PSD), charge density, and functional groups of AC [19]. Depending on the physicochemical features of AC, the uptake of ARGs on AC may differ. One of the most critical properties influencing the adsorption process is the PSD of AC [20]. According to previous studies, the pore size of AC below 15 Å was found to be more effective for the adsorption of small organic micropollutants [21]. Large molecular weight humic substances (1 - 10 kDa) are mostly adsorbed in the mesopores of AC (20 - 500 Å) [22]. The different sizes of AC pores provide varying access routes for molecules. Larger pores accommodate larger molecules, while smaller pores are suitable for smaller molecules. So far, several studies have been focused on the occurrence and removal of ARGs in different treatment processes in DWTP [17] [23] [24]. However, little is known about the accessibility of ARGs on the AC pores and the fate of ARGs during the adsorption process.

Hence, the objectives of this study were to investigate the possible access of the tetracycline resistance gene into the pores of AC and the impact of the PSD of AC on the uptake capacity changes of the gene. For this purpose, batch adsorption experiments were conducted for uptake of *tetG* by eight commercially available ACs (four coal-based and four wood-based) with different PSDs. Experiment data were analyzed using adsorption kinetic and isotherm models. The uptake rate of *tetG* on different types of ACs was determined using adsorption kinetics. The behavior of *tetG* on different types of ACs was described by adsorption isotherms. Furthermore, the correlation analysis between the uptake capacity of the gene and the PSD of AC was performed to evaluate the impact of PSD on the admission of the gene. The concentration of the gene before and after adsorption was quantified using a quantitative polymerase chain reaction (qPCR). This study can serve as a reference in the selection and design of ACs to improve the elimination of

ARGs and reduce the risk of spreading ARGs in DWTP.

2. Materials and Methods

2.1. Activated Carbon

Four coal-based ACs (AC-1, AC-2, AC-3, AC-4) and four wood-based ACs (AC-5, AC-6, AC-7, AC-8) were purchased from the market. These ACs are steam-activated ones and the main difference regarding their physiochemical properties is PSDs. The PSD of each AC was measured by high-resolution Micromeritics 3Flex instrument (Micromeritics 3Flex, USA) based on nitrogen adsorption. The pore volume and pore surface values of the ACs are shown in Table 1 and Table 2, respectively. The pore size region of AC was categorized based on previous studies that investigated the effect of PSD of AC on the adsorption capacity of dissolved organic matter in drinking water sources [25]. The majority of pores are concentrated in the size range below 20 Å for all eight ACs. For AC-2, the total pore volume and surface area are obviously lower than other types of AC, and this AC has more pores in the size region below 10 Å both its pore volume and pore surface.

Further, the functional groups on the surface of the AC were examined by Fourier transform infrared spectroscopy (FTIR). The FTIR spectra of all eight ACs are displayed in Figure 1. The existence of a strong peak at 3500 cm^{-1} indicates the presence of hydroxyl groups. In addition, amide groups and carboxylic acid groups were detected at wavenumbers of 1650 and 1400 cm^{-1}, respectively [26]. All eight ACs had similar functional groups, suggesting these ACs had similar chemical structure. The different properties of all types of ACs were clearly seen in the total surface area, total pore volume and PSD of ACs, demonstrating these properties might contribute more to the uptake of *tetG*.

Table 1. Total pore volume and the pore volume percentages in different pore size regions of eight ACs used in this study.

Activated carbons	AC-1	AC-2	AC-3	AC-4	AC-5	AC-6	AC-7	AC-8
Origin	Coal	Coal	Coal	Coal	Wood	Wood	Wood	Wood
Total pore volume (cm^3/g)	0.69	0.28	0.44	0.55	0.37	0.59	0.62	0.66
Pore size (Å)	**Pore volume (%)**							
0 - 10	36.9	98.1	53.2	43.1	82.8	66.5	52.6	60.5
10 - 20	27.1	0.0	35.7	28.8	13.6	29.6	23.0	35.1
20 - 30	12.5	0.0	3.5	10.4	0.0	0.0	3.7	0.0
30 - 50	9.6	0.0	0.7	7.5	0.0	0.0	6.0	0.5
30 - 100	16.2	0.0	2.1	12.6	0.0	0.7	13.6	1.7
30 - 240	23.5	1.9	7.5	17.6	3.6	3.8	20.7	4.4
50 - 100	6.6	0.0	1.3	5.1	0.0	0.7	7.6	1.2
50 - 240	13.9	1.9	6.7	10.1	3.6	3.8	14.7	4.0

Table 2. Total pore surface area and the surface area percentages in different pore size regions of eight ACs used in this study.

Activated carbons	AC-1	AC-2	AC-3	AC-4	AC-5	AC-6	AC-7	AC-8
Origin	Coal	Coal	Coal	Coal	Wood	Wood	Wood	Wood
Total surface area (cm^2/g)	956	745	820	856	866	1238	1053	1322
Pore size (Å)	**Pore surface (%)**							
0 - 10	72.4	99.9	76.5	73.9	91.9	83.4	81.5	78.2
10 - 20	19.8	0.0	21.9	20.4	8.0	16.4	15.2	21.5
20 - 30	4.3	0.0	1.1	3.3	0.0	0.0	1.0	0.0
30 - 50	2.1	0.0	0.1	1.5	0.0	0.0	1.0	0.1
30 - 100	3.0	0.0	0.3	2.1	0.0	0.1	1.9	0.2
30 - 240	3.4	0.1	0.5	2.4	0.1	0.2	2.3	0.3
50 - 100	0.9	0.0	0.1	0.6	0.0	0.1	0.8	0.1
50 - 240	1.4	0.1	0.4	0.9	0.1	0.2	1.2	0.3

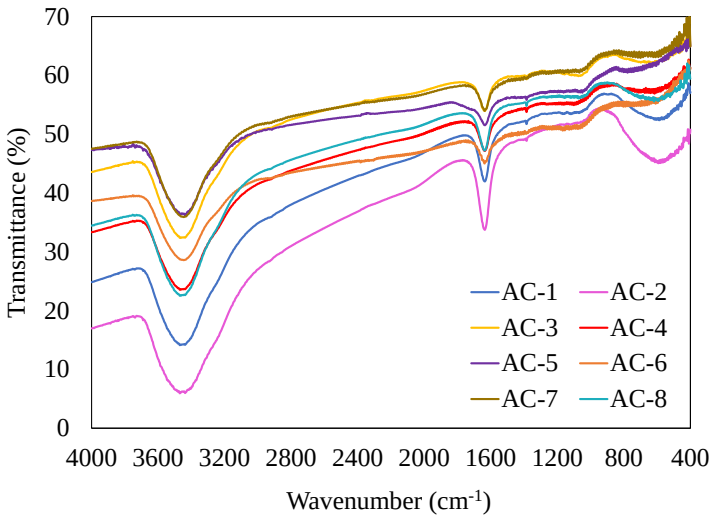

Figure 1. The FTIR spectra of eight ACs used in this study.

2.2. Antibiotic Resistance Genes (ARGs) Preparation

The tetracycline resistance gene (*tetG*) was prepared by referring to the TA cloning method (TaKaRa, Japan). The non-quantitative PCR instrument was used to amplify the target gene. Further, the Gel and PCR Clean-up kit (Macherey-Nagel, Germany) was utilized to purified PCR product. The ligation reaction of the target gene was performed with plasmid pMD20-T (TaKaRa, Japan). The resulting product was transformed into *E. coli* DH5α competent cells and cultured overnight in LB medium with tetracycline. Further, white colonies were picked for PCR amplification to confirm the insert of the target gene. The con-

firmed colonies containing the desired plasmid were cultured overnight in LB medium with tetracycline. Then, the plasmid was extracted from *E. coli* DH5 using a plasmid extraction kit (Macherey-Nagel, Germany), and its concentration was measured using a Quantus Fluorometer. Further, the qPCR analysis was performed to amplify *tetG* at 133 bp with designed primers (forward primer: TTA TCG CCG CCG CCC TTC T, reverse primer: TCA TCC AGC CGT AAC AGA AC) and utilizing SYBR® Premix Ex TaqTM (TaKaRa, Japan) based on the manufacturer's protocol [27]. The amplification product was isolated by gel electrophoresis and purified using a Gel and PCR Clean-up kit. The purified amplification product was diluted with sterile deionized water to obtain the amplicon solution and used for adsorption experiments.

2.3. Adsorption Experiments

Adsorption experiments were carried out using the batch equilibrium technique in 5 mL vials at 20˚C. Adsorption kinetics experiments were conducted for 180 minutes until equilibrium was attained using an AC dose of 1 $g \cdot L^{-1}$ and an initial *tetG* concentration of 6.86×10^{13} copies$\cdot L^{-1}$. Adsorption isotherm experiments were conducted at AC doses within the range of 0.01 - 1 $g \cdot L^{-1}$, and the initial concentration of *tetG* was 6.86×10^{13} copies$\cdot L^{-1}$. After shaking for 180 minutes, centrifugation was performed for 10 minutes at 12,000 g to remove the AC particles. The obtained supernatant was subjected to *tetG* quantification. The concentration of *tetG* before and after adsorption was determined by qPCR.

3. Results and Discussion

3.1. Uptake Rate of *tetG* on ACs

The changes of the uptake rate of *tetG* with time are shown in **Figure 2**. The uptake was rapid at the beginning and gradually slowed as the contact time increased until equilibrium was reached in 150 minutes. For the coal-based ACs, as displayed in **Figure 2(a)**, compared to AC-2, the uptake rate for AC-1, AC-3, and AC-4 was higher, being about 4.04, 3.80, and 3.90 log at 180 min, respectively. AC-2 showed a lower uptake rate, which only reached 0.75 log after 180 min. It was found that uptake rate by AC-2 was approximately 5 times lower than other types of coal-based AC. Further, the uptake rate of *tetG* for wood-based ACs is presented in **Figure 2(b)**. AC-7 had the highest uptake rate of *tetG* (4.50 log) compared to the other wood-based ACs at 180 min. Meanwhile, the uptake rates for AC-5, AC-6, and AC-8 were 3.20, 3.44, and 3.46 logs, respectively. The differences in the uptake rate of *tetG* on AC were attributed to the different surface properties of the ACs, such as surface chemistry, total pore volume, total surface area, etc.

Pseudo-first-order and pseudo-second-order kinetic models were used in this study to determine the uptake rate and possible mechanisms involved in the uptake of *tetG*. The pseudo-first-order kinetic model is given as [28]:

$$\frac{dq_t}{d_t} = k_1\left(q_e - q_t\right) \quad (1)$$

where q_t (copies·mg^{-1}) and q_e (copies·mg^{-1}) are the uptake capacity *of tetG* onto AC at time t and equilibrium, respectively. The k_1 (min^{-1}) and t (min) are the pseudo-first-order rate constant and time of reaction, respectively. The k_1 and q_e were obtained from linear plot of ln (q_e – q_t) with time as displayed in **Figure 3**. Further, the pseudo-second-order kinetic model is exhibited by the following equation [28]:

$$\frac{dq_t}{d_t} = k_2\left(q_e - q_t\right)^2 \quad (2)$$

where k_2 (copies·mg^{-1}·min^{-1}) is the pseudo-second-order rate constant. The k_2 and q_e were computed from the intercept and slope of the linear plot of t/q_t against t as demonstrated in **Figure 4**.

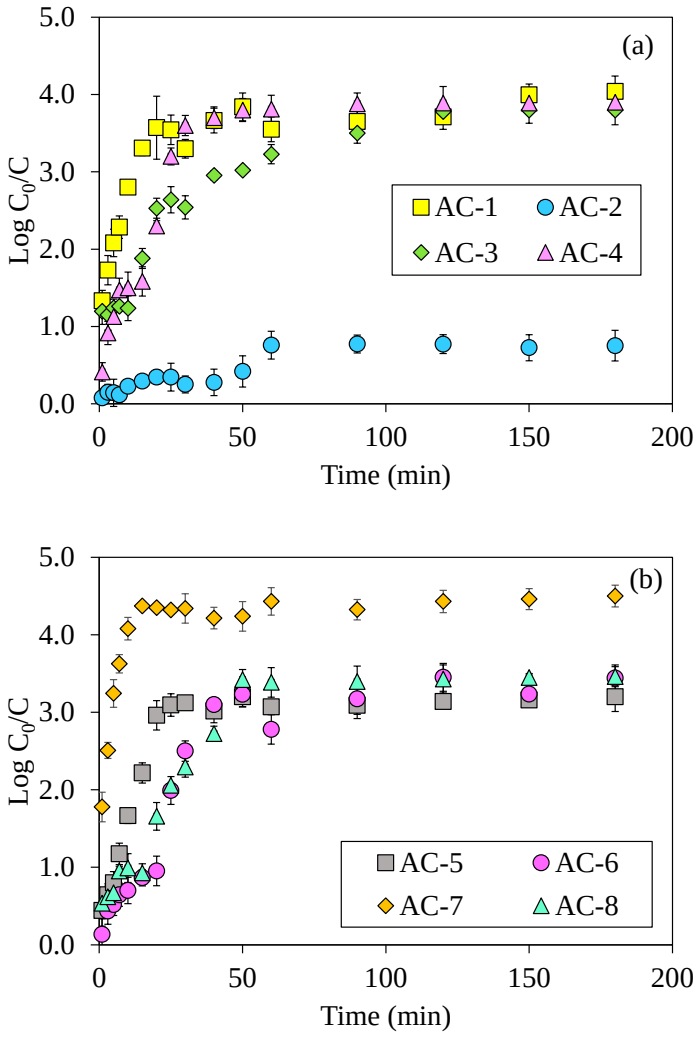

Figure 2. Changes of the uptake rate of *tetG* with time by (a) 4 coal-based and (b) 4 wood-based ACs (AC dose: 1 g·L^{-1}, initial *tetG* concentration: 6.86 × 10^{13} copies·L^{-1}).

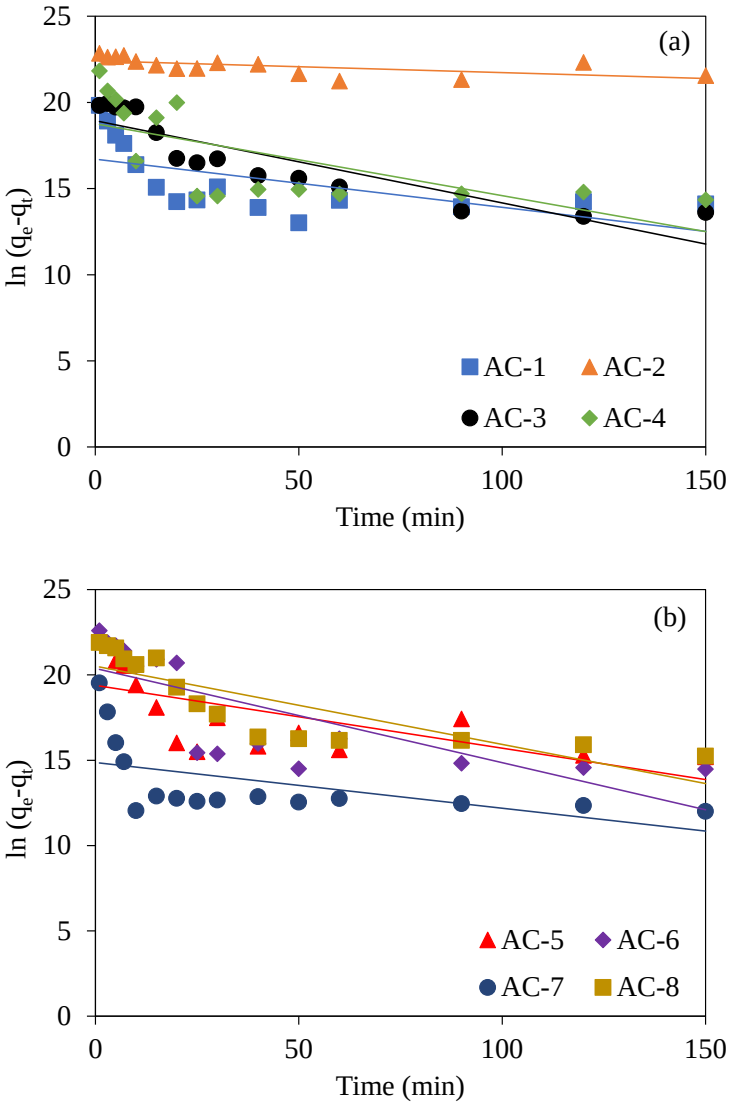

Figure 3. Analysis of the uptake of *tetG* based on the pseudo-first-order kinetic model for (a) coal-based and (b) wood-based ACs.

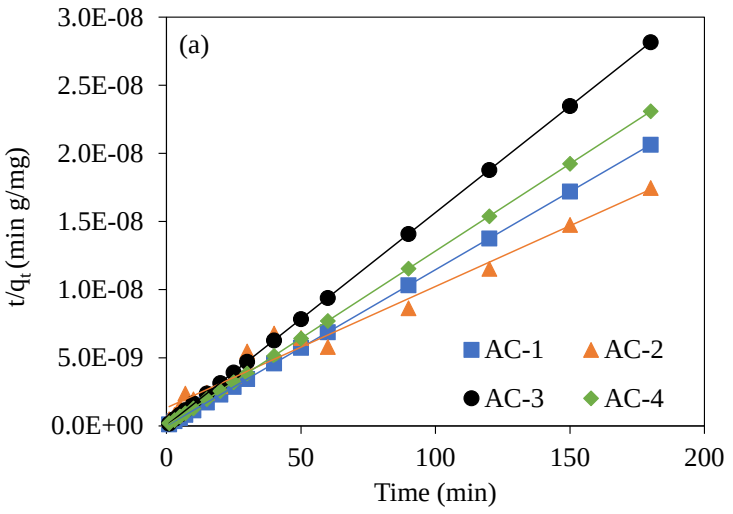

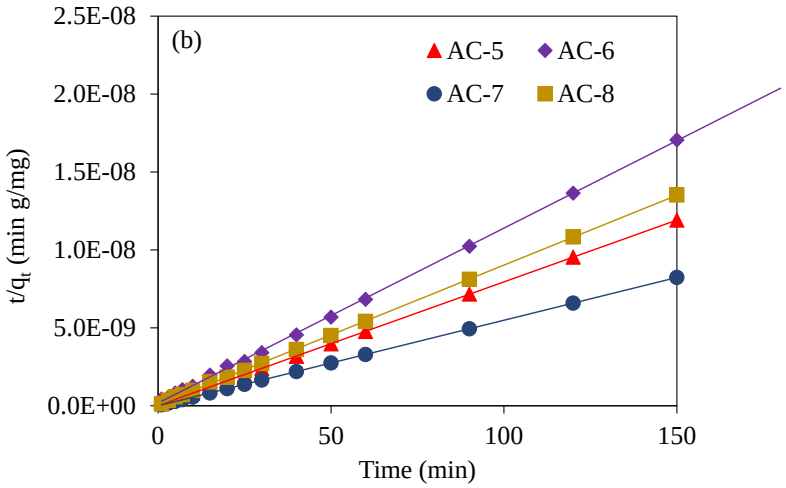

Figure 4. Analysis of the uptake of *tetG* based on the pseudo-second-order kinetic model for (a) coal-based and (b) wood-based ACs.

As shown in **Figure 3** and **Figure 4**, pseudo-second-order fitted well with the experimental data compared to the pseudo-first-order kinetic model, suggesting the experimental data follows the pseudo-second-order reaction. The R^2 value of the pseudo-second-order was very high ($R^2 > 0.975$), and the calculated q_e value was in good agreement with the experimental ones as shown in **Table 3**, indicating the applicability of the pseudo-second-order kinetic model to describe the uptake rate of *tetG* on AC. The highest uptake rate constant was found in AC-1 (4.64×10^{-9} copies·mg^{-1}·min^{-1}) for coal-based AC and AC-7 (1.59×10^{-8} copies·mg^{-1}·min^{-1}) for wood-based one. While AC-2 had the smallest uptake rate constant compared to all types of AC (coal-based and wood-based), which was (5.97×10^{-12} copies·mg^{-1}·min^{-1}). Moreover, as displayed in **Table 3**, the uptake capacity (q_e) of *tetG* for coal-based and wood-based ACs was in the range 6.40×10^9 - 1.12×10^{10} copies·mg^{-1} and 8.91×10^9 - 1.82×10^{10} copies·mg^{-1}, respectively.

The pseudo-second-order reaction assumes that the adsorption process is controlled by chemisorption, involving valence forces by sharing electrons between the adsorbent and the adsorbate [29]. As mentioned earlier, hydroxyl groups and carboxylic acid groups are present in eight ACs. These functional groups may allow for H-bonding interactions between the H atom of the AC and the N atom of the *tetG* DNA base. Moreover, π- π interactions may occur between the aromatic structure of AC and the DNA base of *tetG*. All DNA bases are aromatic and can easily interact with AC through this interaction. AC also consists of aromatic sheets that are flat and broken in places by slit-shaped pores. Heteroatoms (e.g. oxygen, nitrogen) exist in individual particles inserted between the aromatic sheets or incorporated as functional groups [30]. Similar findings were also obtained in other studies [31].

3.2. Uptake Capacity of *tetG* on ACs

The capability of AC to adsorb *tetG* was evaluated with the Freundlich isotherm model. The equation of this model is described as follows [32].

Table 3. Estimated pseudo-second-order kinetic model parameters for the uptake of *tetG* on all eight ACs used in this study.

AC types	Pseudo-second-order parameters		
	k_2 (copies·mg^{-1}·min^{-1})	q_e (copies·mg^{-1})	R^2
AC-1	4.64×10^{-9}	8.73×10^{9}	1.000
AC-2	5.97×10^{-12}	1.12×10^{10}	0.975
AC-3	7.01×10^{-10}	6.40×10^{9}	1.000
AC-4	5.44×10^{-10}	7.81×10^{9}	1.000
AC-5	2.44×10^{-10}	1.26×10^{10}	1.000
AC-6	7.02×10^{-11}	8.91×10^{9}	1.000
AC-7	1.59×10^{-8}	1.82×10^{10}	1.000
AC-8	1.16×10^{-10}	1.12×10^{10}	1.000

$$q_e = K_F C_e^{1/n} \tag{3}$$

where K_F is the Freundlich constant representing the adsorption strength, and *1/n* reflects the affinity of *tetG* with AC.

The Freundlich isotherm data for the uptake of *tetG* on coal-based and wood-based ACs are shown in Figure 5. The Freundlich isotherm parameters and R^2 values are summarized in Table 4. The experimental data for all eight ACs were fitted well with this model, except AC-2. The *1/n* value was found below 1, indicating the uptake of *tetG* on AC is favorable [33]. AC-2 had the highest *1/n* value compared to the other types of ACs. This implies that weak affinity between *tetG* and AC-2 during the adsorption process. Meanwhile, other types of ACs exhibit small *1/n* values compared to AC-2. A smaller *1/n* value indicates a higher level of affinity or a stronger interaction between *tetG* and AC [33]. The K_F values for coal-based and wood-based ACs varied in the range of 1.71×10^3 - 8.00×10^9 (copies·g^{-1})$^{1-1/n}$ and 7.00×10^8 - 3.00×10^{10} (copies·g^{-1})$^{1-1/n}$, respectively. The highest K_F value was found from AC-1 and AC-7 for coal based and wood-based AC, respectively. Compared to all types of ACs, AC-2 possessed the smallest K_F value. The K_F value follows the order AC-7 > AC-1 > AC-5 > AC-6 > AC-4 > AC-8 > AC-3 > AC-2. While the *1/n* value follows the order AC-2 > AC-3 > AC-4 > AC-8 > AC-5 > AC-6 > AC-1 > AC-7. Generally, wood-based ACs were found to have a higher K_F value than coal-based ACs, indicating wood-based ACs have a higher ability to accept ARGs compared to coal-based ones.

3.3. Correlation Analysis of the Relations of the Uptake Capacity of *tetG* with Pore Volume and Pore Surface in Different Size Regions of ACs

Table 5 shows the Pearson correlation analysis between the estimated K_F and the pore volume as well as the pore surface in different pore size regions of eight

ACs. The highest positive correlation was noticed between K_F and the pore size region of 50 - 100 Å in both pore volume and pore surface, suggesting pores within this size region might be effective for the uptake of *tetG*. Pores in the range of 50 - 100 Å probably provide ideal accessibility for *tetG*, allowing the gene to enter and be fixed inside the pore. Pore sizes of 50 - 240 Å also generated a good positive relation with K_F but the correlation coefficient was slightly smaller compared to pores of 50 - 100 Å. It indicated that *tetG* is preferentially adsorbed on pores slightly larger than its size due to the greater attractive force and more contact points between *tetG* and the active site of AC. This result is attributed to the potential force overlap formed when the opposite pore wall is slightly larger than the size of the adsorbed molecule [34]. Pore sizes of 50 - 240 Å may be able to adsorb *tetG*, but the available active sites for uptake are smaller due to the limited surface area at larger pore sizes.

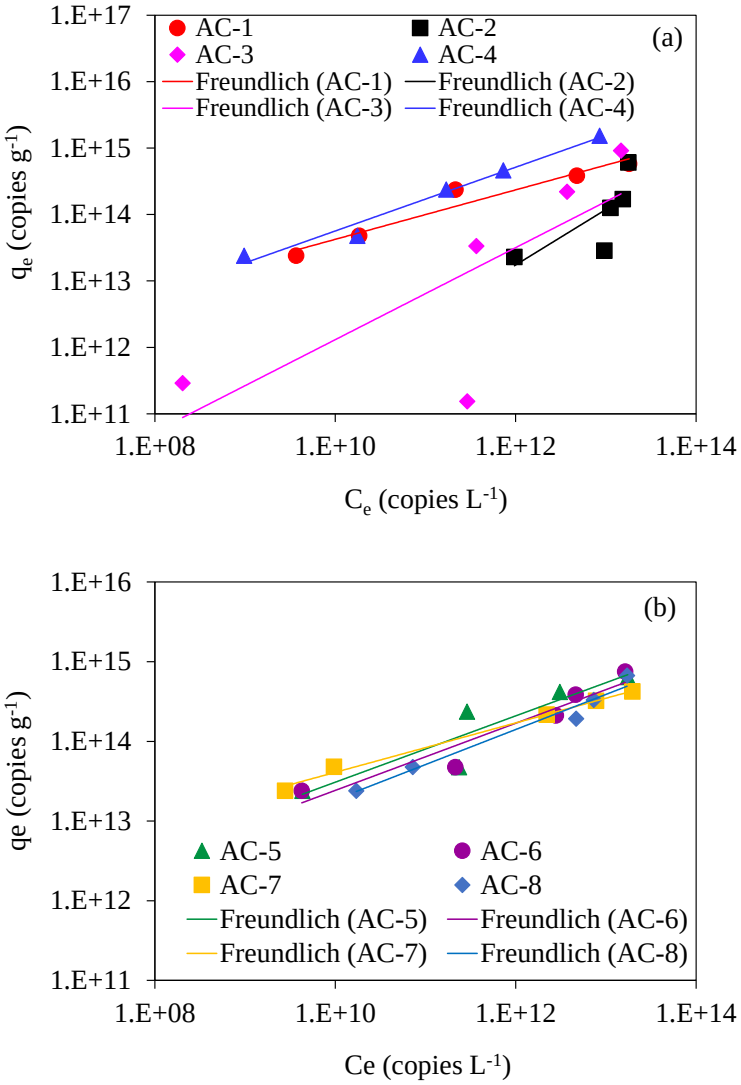

Figure 5. Analysis of the uptake capacity of *tetG* based on the Freundlich isotherm model for (a) 4 coal-based and (b) 4 wood-based ACs.

Table 4. Estimated Freundlich isotherm model parameters for the uptake capacity of *tetG* on all eight ACs used in this study.

AC types	K_F (copies·g^{-1})$^{1-1/n}$	*1/n*	R^2
AC-1	8.00×10^9	0.37	0.949
AC-2	1.71×10^3	0.83	0.502
AC-3	1.55×10^5	0.69	0.981
AC-4	9.00×10^8	0.48	1.000
AC-5	2.00×10^9	0.42	0.914
AC-6	1.00×10^9	0.42	0.960
AC-7	3.00×10^{10}	0.31	0.999
AC-8	7.00×10^8	0.44	0.903

Table 5. Pearson correlation coefficient (*r*) obtained from the correlation analysis of the estimated K_F with the pore volume and pore surface in different pore size regions of eight ACs. The symbol "-" indicates the correlation is negative.

Pore size (Å)	Pore volume	Pore surface
0 - 10	−0.302	−0.132
10 - 20	−0.015	0.045
20 - 30	0.165	0.131
30 - 50	0.467	0.395
30 - 100	0.599	0.490
30 - 240	0.629	0.509
50 - 100	0.744	0.670
50 - 240	0.733	0.652
Total pore volume	0.383	0.383
Total surface area	0.139	0.139

Pore sizes below 20 Å showed a negative correlation with K_F as displayed in Table 5, indicating these pore sizes are not accessible by *tetG*. Hence, it is obvious that AC-2 has the lowest K_F value compared to other types of ACs due to more pore sizes in the size region below 20 Å, with the percentage of pore volume and pore surface being 98.1% and 99.9%, respectively (Table 1 and Table 2). The size exclusion effect might prevent *tetG* from entering the pores of AC-2. Thus, the accessibility of *tetG* to the AC pores is crucial since the appropriate pore size can allow the penetration of *tetG* into the pore, resulting in more effective gene uptake. This result showed that micropores (<20 Å) were less effective for the uptake of *tetG* [35]. The micropore may have a larger surface area but it has no entry point and insufficient transport pathways for the gene.

4. Conclusion

The possible access of *tetG* and the impact of the PSD of AC on the uptake of

tetG were evaluated. The results suggested that the uptake of *tetG* varied greatly with the type of AC. The uptake kinetic analysis indicated that the uptake of *tetG* followed pseudo-second-order reaction. The uptake capacity analysis demonstrated that the Freundlich isotherm model described the uptake capacity data quite well. In addition, correlation analysis between the estimated K_F value and PSD of ACs suggested that pores with sizes of 50 - 100 Å were more effective in uptake of *tetG*. Pores below 20 Å were too small for the uptake of *tetG*. This study can serve as a reference for AC selection or material design for optimizing the uptake of *tetG* from water.

Acknowledgements

This study was conducted with the support of JSPS for Grant-in-Aid for Scientific Research (A) (20H00261).

Conflicts of Interest

The authors declare no conflicts of interest regarding the publication of this paper.

References

[1] Li, S., Zhang, C., Li, F., Hua, T., Zhou, Q. and Ho, S.-S. (2021) Technologies towards Antibiotic Resistance Genes (ARGs) Removal from Aquatic Environment: A Critical Review. *Journal of Hazardous Materials*, **411**, Article 125148. https://doi.org/10.1016/j.jhazmat.2021.125148

[2] Davies, J. and Davies, D. (2010) Origins and Evolution of Antibiotic Resistance. *Microbiology and Molecular Biology Reviews*, **74**, 417-433. https://doi.org/10.1128/MMBR.00016-10

[3] Li, B., Qiu, Y., Song, Y., Lin, Y., Lin, H. and Yin, H. (2019) Dissecting Horizontal and Vertical Gene Transfer of Antibiotic Resistance Plasmid in Bacterial Community using Microfluidics. *Environment International*, **131**, Article 105007. https://doi.org/10.1016/j.envint.2019.105007

[4] Kumar, S.B., Arnipalli, S.R. and Ziouzenkova, O. (2020) Antibiotics in Food Chain: The Consequences for Antibiotic Resistance. *Antibiotics*, **9**, Article 688. https://doi.org/10.3390/antibiotics9100688

[5] Tian, Y., Yao, S., Zhou, L., Hu, Y., Lei, J., Wang, L., Zhang, J., Liu, Y. and Zui, C. (2022) Efficient Removal of Antibiotic-Resistant Bacteria and Intracellular Antibiotic Resistance Genes by Heterogeneous Activation of Peroxymonosulfate on Hierarchical Macro-Mesoporous Co_3O_4-SiO_2 with Enhanced Photogenerated Charges. *Journal of Hazardous Materials*, **430**, Article 127414. https://doi.org/10.1016/j.jhazmat.2021.127414

[6] Sanganyado, E. and Gwenzi, W. (2019) Antibiotic Resistance in Drinking Water Systems: Occurrence, Removal, and Human Health Risks. *Science of the Total Environment*, **669**, 785-797. https://doi.org/10.1016/j.scitotenv.2019.03.162

[7] Chu, G., Qi, W., Chen, W., Zhang, Y., Gao, S., Wang, Q., Gao, C. and Gao, M. (2024) Metagenomic Insights into the Nitrogen Metabolism, Antioxidant Pathway, and Antibiotic Resistance Genes of Activated Sludge from a Sequencing Batch Reactor under Tetracycline Stress. *Journal of Hazardous Materials*, **462**, Article

132788. https://doi.org/10.1016/j.jhazmat.2023.132788

[8] Chen, J., Su, Z., Dai, T., Huang, B., Mu, Q., Zhang, Y. and Wen, D. (2019) Occurrence and Distribution of Antibiotic Resistance Genes in the Sediments of the East China Sea bays. *Journal of Environmental Sciences*, **81**, 156-167. https://doi.org/10.1016/j.jes.2019.01.016

[9] Lu, J., Zhang, Y., Wu, J., Wang, J., Zhang, C. and Lin, Y. (2019) Occurrence and Spatial Distribution of Antibiotic Resistance Genes in the Bohai Sea and Yellow Sea Areas, China. *Environmental Pollution*, **252**, 450-460. https://doi.org/10.1016/j.envpol.2019.05.143

[10] Cheng, J., Yang, Y., Liu, Y., Tang, M., Wang, R., Tian, Y. and Jia, C. (2019) Bacterial Community Shift and Antibiotics Resistant Genes Analysis in Response to Biodegradation of Oxytetracycline in Dual Graphene Modified Bioelectrode Microbial Fuel Cell. *Bioresource Technology*, **276**, 236-243. https://doi.org/10.1016/j.biortech.2019.01.006

[11] Jones, R.N., Flonta, M., Gurler, N., Cepparulo, M., Mendes, R. and Castanheira, M. (2014) Resistance Surveillance Program Report for Selected European Nations (2011). *Diagnostic Microbiology and Infectious Disease*, **78**, 429-436. https://doi.org/10.1016/j.diagmicrobio.2013.10.008

[12] Zhang, L., Ji, L., Liu, X., Zhu, X., Ning, K. and Wang, Z. (2022) Linkage and Driving Mechanisms of Antibiotic Resistome in Surface and Ground Water: Their Responses to Land Use and Seasonal Variation. *Water Research*, **215**, Article 118279. https://doi.org/10.1016/j.watres.2022.118279

[13] Huang, L., Xu, Y., Xu, J., Ling, J., Zheng, L., Zhou, X. and Xie, G. (2019) Dissemination of Antibiotic Resistance Genes (ARGs) by Rainfall on a Cyclic Economic Breeding Livestock Farm. *International Biodeterioration & Biodegradation*, **138**, 114-121. https://doi.org/10.1016/j.ibiod.2019.01.009

[14] Szekeres, E., Baricz, A., Chiriac, C.M., Farkas, A., Opris, O., Soran, M.-L., Andrei, A.-S., Rudi, K., Balcázar, J.L., Dragos, N. and Coman, C. (2017) Abundance of Antibiotics, Antibiotic Resistance Genes and Bacterial Community Composition in Wastewater Effluents from Different Romanian Hospitals. *Environmental Pollution*, **225**, 304-315. https://doi.org/10.1016/j.envpol.2017.01.054

[15] Rafraf, I.D., Lekunberri, I., Sànchez-Melsió, A., Aouni, M., Borrego, C.M. and Balcázar, J.L. (2016) Abundance of Antibiotic Resistance Genes in Five Municipal Wastewater Treatment Plants in the Monastir Governorate, Tunisia. *Environmental Pollution*, **219**, 353-358. https://doi.org/10.1016/j.envpol.2016.10.062

[16] Su, H.-C., Liu, Y.-S., Pan, C.-G., Chen, J., He, L.-Y. and Ying, G.-G. (2018) Persistence of Antibiotic Resistance Genes and Bacterial Community Changes in Drinking Water Treatment System: From Drinking Water Source to Tap Water. *Science of the Total Environment*, **616-617**, 453-461. https://doi.org/10.1016/j.scitotenv.2017.10.318

[17] Xu, L., Canales, M., Zhou, Q., Karu, K., Zhou, X., Su, J., Campos, L.C. and Ciric, L. (2023) Antibiotic Resistance Genes and the Association with Bacterial Community in Biofilms Occurring during the Drinking Water Granular Activated Carbon (GAC) Sandwich Biofiltration. *Journal of Hazardous Materials*, **460**, Article 132511. https://doi.org/10.1016/j.jhazmat.2023.132511

[18] Hu, Y., Zhang, T., Jiang, L., Luo, Y., Yao, S., Zhang, D., Lin, K. and Cui, C. (2019) Occurrence and Reduction of Antibiotic Resistance Genes in Conventional and Advanced Drinking Water Treatment Processes. *Science of the Total Environment*, **669**, 777-784. https://doi.org/10.1016/j.scitotenv.2019.03.143

[19] Anggreini, S., Rosadi, M.Y., Yamada, T., Hudori, H., Deng, Z. and Li, F. (2023) Characteristics of Organic Matter released from Drinking Water Treatment Sludge under Different Storage Conditions: Evaluation Based on Activated Carbon Adsorbability. *Chemosphere*, **339**, Article 139679. https://doi.org/10.1016/j.chemosphere.2023.139679

[20] Li, F., Yuasa, A., Chiharada, H. and Matsui, Y. (2003) Polydisperse Adsorbability Composition of Several Natural and Synthetic Organic Matrices. *Journal of Colloid and Interface Science*, **265**, 265-275. https://doi.org/10.1016/S0021-9797(03)00526-5

[21] Ebie, K., Li, F., Azuma, Y., Yuasa, A. and Hagishita, T. (2001) Pore Distribution Effect of Activated Carbon in Adsorbing Organic Micropollutants from Natural Water. *Water Research*, **35**, 167-179. https://doi.org/10.1016/S0043-1354(00)00257-8

[22] Golea, D.M., Jarvis, P., Jefferson, B., Moore, G., Sutherland, S., Parsons, S.A. and Judd, S.J. (2020) Influence of Granular Activated Carbon Media Properties on Natural Organic Matter and Disinfection By-Product Precursor Removal from Drinking Water. *Water Research*, **174**, Article 115613. https://doi.org/10.1016/j.watres.2020.115613

[23] Sun, L., Ding, Y., Yang, B., He, N. and Chen, T. (2020) Effect of Biological Powdered Activated Carbon on Horizontal Transfer of Antibiotic Resistance Genes in Secondary Effluent. *Environmental Engineering Science*, **37**, 365-372. https://doi.org/10.1089/ees.2019.0397

[24] Sun, L., Shi, P., He, N., Zhang, Q. and Duan, X. (2019) Antibiotic Resistance Genes Removal and Membrane Fouling in Secondary Effluents by Combined Processes of PAC/BPAC-UF. *Journal of Water and Health*, **17**, 910-920. https://doi.org/10.2166/wh.2019.160

[25] Li, F., Yuasa, A., Ebie, K., Azuma, Y., Hagishita, T. and Matsui, Y. (2002) Factors Affecting the Adsorption Capacity of Dissolved Organic Matter onto Activated Carbon: Modified Isotherm Analysis. *Water Research*, **36**, 4592-4604. https://doi.org/10.1016/S0043-1354(02)00174-4

[26] Tan, Y.L., Islam, M.A., Asif, M. and Hameed, B.H. (2014) Adsorption of Carbon Dioxide by Sodium Hydroxide-Modified Granular Coconut Shell Activated Carbon in a Fixed Bed. *Energy*, **77**, 926-931. https://doi.org/10.1016/j.energy.2014.09.079

[27] Li, W., Li, J., Bhat, S.A., Wei, Y., Deng, Z. and Li, F. (2021) Elimination of Antibiotic Resistance Genes from Excess Activated Sludge Added for Effective Treatment of Fruit and Vegetable Waste in a Novel Vermireactor. *Bioresource Technology*, **325**, 124695. https://doi.org/10.1016/j.biortech.2021.124695

[28] Agarwal, S. and Rani, A. (2017) Adsorption of Resorcinol from Aqueous Solution onto CTAB/NaOH/Flyash Composites: Equilibrium, Kinetics and Thermodynamics. *Journal of Environmental Chemical Engineering*, **5**, 526-538. https://doi.org/10.1016/j.jece.2016.11.035

[29] Li, S., Li, Z., Ke, B., He, Z., Cui, Y., Pan, Z., Li, D., Huang, S., Lai, C. and Su, J. (2019) Magnetic Multi-Walled Carbon Nanotubes Modified with Polyaluminium Chloride for Removal of Humic Acid from Aqueous Solution. *Journal of Molecular Liquids*, **279**, 241-250. https://doi.org/10.1016/j.molliq.2019.01.016

[30] Li, N., Ma, X., Zha, Q., Kim, K., Chen, Y. and Song, C. (2011) Maximizing the Number of Oxygen-Containing Functional Groups on Activated Carbon by using Ammonium Persulfate and Improving the Temperature-Programmed Desorption Characterization of Carbon Surface Chemistry. *Carbon*, **49**, 5002-5013. https://doi.org/10.1016/j.carbon.2011.07.015

[31] Yu, W., Zhan, S., Shen, Z., Zhou, Q. and Yang, D. (2017) Efficient Removal Me-

chanism for Antibiotic Resistance Genes from Aquatic Environments by Graphene Oxide Nanosheet. *Chemical Engineering Journal*, **313**, 836-846. https://doi.org/10.1016/j.cej.2016.10.107

[32] Varga, M., ELAbadsa, M., Tatár, E. and Mihucz, V.G. (2019) Removal of Selected Pharmaceuticals from Aqueous Matrices with Activated Carbon under Batch Conditions. *Microchemical Journal*, **148**, 661-672. https://doi.org/10.1016/j.microc.2019.05.038

[33] Kalam, S., Abu-Khamsin, S.A., Kamal, M.S. and Patil, S. (2021) Surfactant Adsorption Isotherms: A Review. *ACS Omega*, **6**, 32342-32348. https://doi.org/10.1021/acsomega.1c04661

[34] Pelekani, C. and Snoeyink, V.L. (1999) Competitive Adsorption in Natural Water: Role of Activated Carbon Pore Size. *Water Research*, **33**, 1209-1219. https://doi.org/10.1016/S0043-1354(98)00329-7

[35] Hu, Z. and Srinivasan, M.P. (2001) Mesoporous High-Surface-Area Activated Carbon. *Microporous and Mesoporous Materials*, **43**, 267-275. https://doi.org/10.1016/S1387-1811(00)00355-3